Article

Accurate Isomerization Enthalpy and Investigation of the Errors in Density Functional Theory for DHA/VHF Photochromism Using Diffusion Monte Carlo

Kayahan Saritas, and Jeffrey C. Grossman

J. Phys. Chem. C, **Just Accepted Manuscript** • DOI: 10.1021/acs.jpcc.7b09437 • Publication Date (Web): 08 Nov 2017

Accurate Isomerization enthalpy and Investigation of the Errors in Density Functional Theory for DHA/VHF Photochromism Using Diffusion Monte Carlo

Kayahan Saritas* and Jeffrey C. Grossman*

Department of Materials Science and Engineering, Massachusetts Institute of Technology, Cambridge, MA, 02139

E-mail: kayahan@mit.edu; jcg@mit.edu
Phone: +1 (0)617 2588741

Abstract

We investigate the isomerization enthalpy of the Dihydroazulene/Vinylheptafulvene (DHA/VHF) molecular photoswitch system derivatives using electronic structure calculation methods including Density Functional Theory (DFT), Quantum Monte Carlo (QMC) and Coupled Cluster (CCSD(T)). Recent efforts have focused on tuning the isomerization enthalpy of the photoswitch for solar thermal energy storage applications using substitutional functional groups on its five and seven membered carbon rings, predominantly using DFT for the energy predictions. However, using the higher accuracy QMC and CCSD(T) methods, we show that in many cases DFT incorrectly predicts the isomerization enthalpy and the errors depends on the functional groups substituted and the choice of the DFT functional. Isomerization of the DHA to VHF molecule is a ring-opening reaction on the five membered ring of the DHA isomer. We find that the DFT errors are correlated to the ring-opening reactions of cyclobutene and cyclo-1,3-hexadiene, such that the DFT error changes monotonically with the size of the carbon ring, although QMC and CCSD(T) results are in a good agreement irrespective of the ring size. Using the QMC and CCSD(T) isomerization enthalpies, we predict gravimetric energy densities of the DHA derivatives for solar thermal storage applications. Our results show that suitable substitutions on DHA can yield gravimentric storage densities as large as 732 kJ/kg.

1 Introduction

Photoswitchable molecules undergo light induced isomerization that changes their physical properties including light absorption properties, electrical conductivities and refractive indexes.[1–4] Among the many characterized photoswitches,[4] azobenzene[5–9] and norbornadiene[10–13] have recently gained renewed interest as a renewable, closed-cycle solar thermal storage material. All photoswitchable molecules can be considered as a potential solar thermal storage material, with the key metrics being: large isomerization enthalpy (ΔH), small molecular weight (or volume), well separated optical absorption bands for the photo-isomers, high forward quantum yield and high fatigue resistance.[5]

Compared to the well studied photoswitches, the dihydzoazulene/vinylheptafulvene (DHA / VHF) couple holds great promise for its application as a solar thermal energy storage material, thanks to its light absorption proper-

ties. The maximum optical absorption band is around 360 nm for DHA and 470 nm for VHF.[14] As shown in Figure 1, DHA, **1a**, undergoes a ring opening reaction to form *s-cis*-vinylheptafulvene (*s-cis*-VHF, **1c**). Then *s-cis*-VHF can convert to *s-trans*-vinylheptafulvene (*s-trans*-VHF, **1e**) via a cis-trans isomerization. The conversion from DHA to VHF is an example of one-way photochromism meaning that the forward reaction can be photoinduced while the reverse reaction proceeds only with thermal activation.[15,16] This strictly one-way photochromism is due to a conical intersection near the *s-cis*-VHF conformation between the ground and first excited states which leads to high forward quantum yields.[16]

DHA/VHF derivatives can be a more efficient solar thermal storage material than azobenzene, due to its favorable quantum yield. In DHA, the forward (ring opening) reaction can occur with a high quantum yield measured from 0.1 to 0.6 at room temperature, depending on the substitutions. In comparison, the trans to cis quantum yield of free azobenzene molecule in solution is nearly 0.2,[17] but it can further be reduced up to 15-fold in highly packed environments.[18] It was shown that when azobenzene and DHA molecules are packed on Au{111} surface and compared for their conversion efficiencies under identical conditions, azobenzene molecules yielded an order of magnitude lower conversion efficiency compared to DHA molecules.[19]

A number of experimental[14,15,20–23] and computational[13,24–26] efforts have focused on tuning the switching properties of DHA/*s-trans*-VHF system with the attachment of functional groups. Although the absorption properties of both of the isomers, the reverse activation energies of the metastable isomers and the photoswitching fatigue resistances have been studied experimentally, to our knowledge, there has been no effort to quantify their ΔH using experimental techniques.

Density functional theory[28,29] (DFT) is a widely used computational method to predict the optical and thermodynamic properties of bulk and molecular systems including molecular photoswitches. In DFT, electron-electron interactions are treated in a mean-field manner using the exchange-correlation interactions. Despite the approximate treatment of the exchange-correlation functional, DFT calculations can usually be useful in identifying the important energetic trends between similar structures. However, Olsen et al.[24] showed that, among the DFT functionals they investigated, M06-2X[30] is the only functional that provides qualitatively correct results for the iΔH of DHA/VHF. They also showed that the B3LYP[31] functional yields a qualitatively inaccurate ordering, as also noted in other works investigating different DHA derivatives.[20] In addition to these results, we find that the PBE[32] functional predicts DHA and *s-trans*-VHF to be nearly isoenergetic (see Table 1). The discrepancies between the DFT results is further calling into question the accuracy of DFT calculations for these compounds. Beyond determining which functionals provide quantitative or qualitative accuracy, it is also of interest to understand why a given DFT functional is predictive or not for their ΔH.

In cases where DFT accuracy is questionable, the physical properties of interest can be calculated with many body methods where electron correlation is treated explicitly. Quantum Monte Carlo[33,34] (QMC) refers to a family of statistical methods for approximating a solution to the many-body Schrödinger equation in a way that explicitly accounts for both the antisymmetry of the many-body wavefunction (exchange) and electron correlation. Although QMC is a high accuracy alternative to DFT,[35] it is computationally much more expensive. QMC has a scaling of $O(N^3)$, where N is the number of electrons, similar to DFT, but the scaling prefactor is nearly 1000 times larger. Another high accuracy approach that can be applicable for these systems and properties is coupled cluster with singles, doubles and non-iterative triples,[36] CCSD(T). CCSD(T) is known as the "gold standard" for quantum chemistry calculations. However, application of CCSD(T) calculations is usually limited to smaller molecules due to its scaling of $O(N^7)$. Therefore, in the absence of quantitative experimental data for the DHA/VHF isomerization

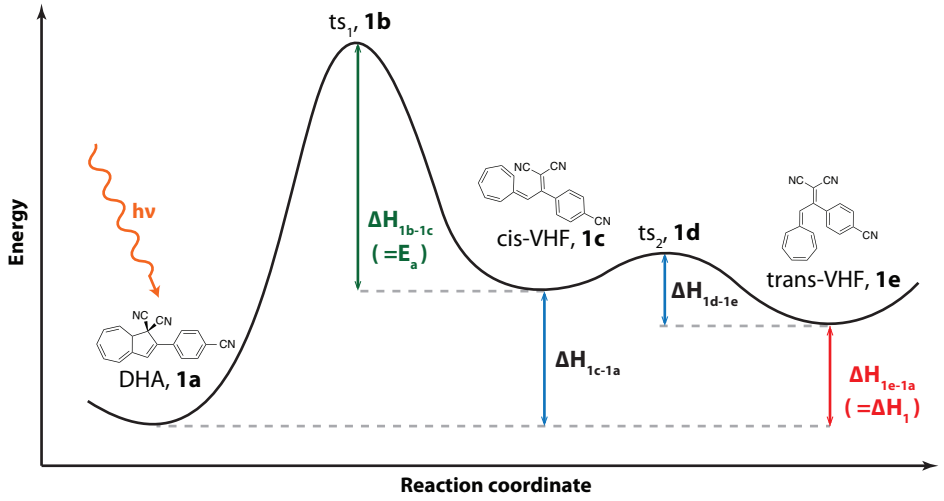

Figure 1: Ground state potential energy surface for the DHA/VHF photoswitch system. Ground state, metastable state and transition state structures are enumerated from **1a** to **1e**. ΔH_1 is the energy difference between the ground state and lowest energy metastable state, DHA and *s-trans*-VHF. ΔE_a is the back reaction activation barrier.

Table 1: Energy differences in vacuum at 0 K for the structures on the ground state potential energy surface (given in Figure 1) of DHA/VHF isomerization.

	HF	LDA	PBE	B3LYP	PBE0	M06-2X	CAM-B3LYP	wB97XD	DMC	Exp.
ΔH_{1a-1c}	0.45	0.37	0.09	0.02	0.33	0.24	0.33	0.43	0.41(6)	
ΔH_{1e-1c}	-0.11	-0.03	-0.07	-0.07	-0.07	-0.06	-0.06	-0.07	-0.09(6)	
ΔH_1	0.34	0.34	0.02	-0.05	0.26	0.18	0.27	0.36	0.32(6)	> 0[15]
E_a	1.48	0.83	0.96	1.11	1.1	1.15	1.25	1.24	1.31(6)	1.39[27]

enthalpy, QMC and CCSD(T) methods can be used to assess the accuracy of DFT methods.

In this work, we therefore investigate DHA/VHF isomerization using both the QMC and CCSD(T) methods to benchmark and analyze the DFT results. On the basis of these results, we address several questions such as (1) What chemical transformations on the ground state potential energy surface of DHA/*s-trans*-VHF isomerization are responsible from the errors in the ΔH? (2) Are these DFT errors in the ΔH only present in DHA/VHF isomers or do they translate to other molecules that also undergo ring opening isomerizations? (3) How does DFT perform when different substitutions are performed on the DHA/VHF system? (4) What energy component of the B3LYP and PBE functionals are responsible for the given ΔH errors?

The paper is organized as follows: In Sec. 2 we summarize the computational details of the performed calculations. In Sec. 3 we present and discuss our results. Specifically, in Sec. 3.1, benchmark calculations are presented using DFT, CCSD(T) and DMC methods on the DHA/VHF isomer. In Sec. 3.2.1, the DFT errors in DHA/VHF isomerization is compared to the ring-opening isomerizations in cyclobutene and 1,3-cyclohexadiene. Sec. 3.3 focuses on the effect of the substitutions on the DFT errors in DHA/VHF isomerization, whereas in Sec. 3.4 we investigate which component of the DFT functionals lead to inaccurate results and in Sec. 3.5 we discuss the energy storage capacity of DHA derivatives for solar thermal storage applications. Sec. 4 comprises summary and conclusions.

2 Computational Methods

DFT calculations[29–32,37–39] are performed as implemented in the Gaussian 09[40] code using an all electron gaussian basis. We report DFT, QMC and CCSD(T) energies at 0K in vacuum, without zero point energy contributions. Geometries of all DHA derivatives investigated in this work are optimized starting from the experimental coordinates obtained from X-ray diffraction[41] of the DHA derivative given in Figure 1, using the 6-31+G* basis. However, the final DFT energies are reported after single point calculations with the 6-311++G** basis. A transition state search is performed using the Berny algorithm.[42] Internal reaction coordinate calculations are performed, starting from the transition state, to confirm that the resulting reaction path starting from the transition state leads to both reactants and products. For each DFT method investigated in this work, geometries are optimized within each method. However, when components of the total energies are investigated (in Sec. 3.4) and for QMC and CCSD(T) calculations, the coordinates optimized with the B3LYP functional are used. In previous studies, B3LYP functional has been shown to yield accurate geometries for DHA/VHF derivatives.[24] CCSD(T) calculations are performed with the frozen core approximation using an aug-cc-pvdz basis and extrapolated to the basis set limit using the MP2[43] aided extrapolation recipe by Truhlar,[44] as the sizes of the molecules were too large to perform triple or quadruple zeta basis calculations at the CCSD(T) level. CCSD(T) and MP2 calculations are performed with the NWCHEM[45] package.

The ΔH of the DHA/VHF isomerization can depend on the solvent polarity, therefore any solvation effects must be considered in the calculations to make more reliable comparison with respect to experimental results. Using DFT and an implicit solvation method,[46] Olsen et al. showed that polar solvents, for example acetonitrile, increase the stability of *s-trans*-VHF more strongly compared to DHA.[24] Experimentally, DHA is known to be more stable than VHF when acetonitrile is used as the solvent, therefore under vacuum, it is expected that the sign of the ΔH remains the same. In the Supplementary Information(SI), Figure S3, we also find that ΔH of DHA/VHF isomerization changes at an almost uniform quantity with the implicit solvation method, when different DFT functionals are benchmarked. Since the added solvation energy depends only weakly on the DFT functionals, in order to understand the errors in DFT methods, their energies can be benchmarked against QMC and CCSD(T) results calculated at the vacuum conditions.

We perform QMC calculations in three main steps. First, we obtain trial wave functions in the form of Slater determinants from the single particle orbitals of the DFT calculations. Second, the trial wavefunction is optimized using variational Monte Carlo (VMC) to obtain a parameterized form of many body trial wavefunction with Jastrow factors. VMC calculations can typically recover 60-90% of the total valence correlation energy.[50] Third, diffusion Monte Carlo (DMC) calculations are carried out to recover the remaining correlation energy and provide highly accurate thermochemistry results. High energy electronic configurations are filtered out in the infinite time limit through the Monte Carlo ensemble, hence the true many-body ground state is obtained. All QMC calculations mentioned in this work are performed at the DMC level, using the CASINO package.[51] We test multiple scenarios where different DFT methods are used to optimize molecular geometries and Slater determinants, and find differences in the ΔH to be no larger than 0.05 eV, indicating that there is efficient error cancellation in the fixed node approximation of DMC wavefunctions. We generate trial wavefunctions, $\Psi_T(R)$, using PBE with Burkatzki-Filippi-Dolg pseudopotentials.[52] DMC calculations are performed using a 0.01 a.u time step and the Casula T-move scheme[53] with a symmetric branching algorithm. An statistical error bar of 0.001 Ha (0.027 eV) is achieved in each DMC calculation, such that a typical DMC run for the molecules considered here takes slightly longer than 50000 steps using 2400 walkers.

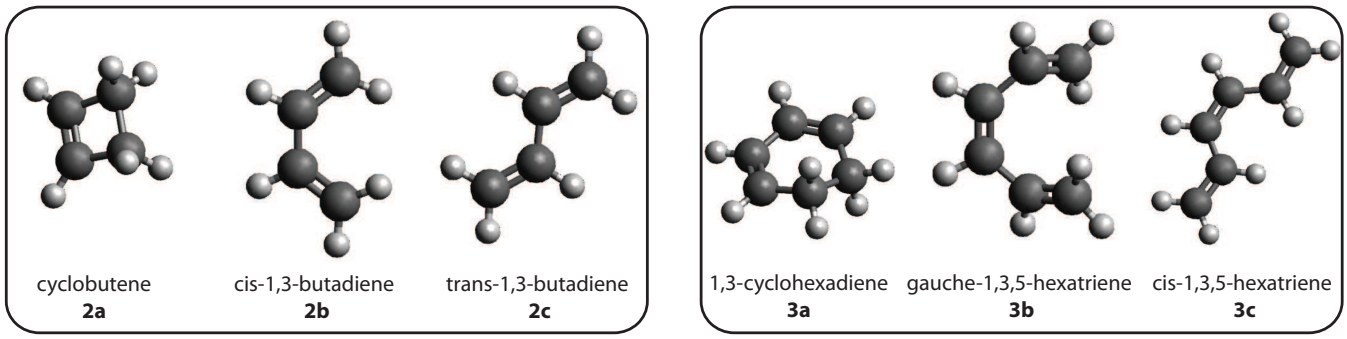

Figure 2: Cyclobutene, **2a-c**, and 1,3-cyclohexadiene, **3a-c** isomers studied in this work. Through the ring opening isomerization reaction, cyclobutene converts into *s-trans*-1,3-butadiene, whereas 1,3-cyclohexadiene converts into *s-cis*-1,3,5-hexatriene.

Table 2: Energy differences (in eV) between the isomers of cyclobutene and 1,3-cyclohexadiene on the ground state potential energy surface of ring opening isomerizations.

	HF	LDA	PBE	B3LYP	PBE0	M06	CAM-B3LYP	TPSSH	DMC	CCSD(T)	Exp.
Cyclobutene, **2a**											
ΔH_{2c-2b}	0.138	0.151	0.157	0.153	0.147	0.128	0.132	0.154	0.14(6)		
ΔH_{2c-2a}	0.636	0.199	0.418	0.616	0.326	0.392	0.494	0.427	0.46(5), 0.53(1)[47]	0.482, 0.479[48]	0.458(6)[47]
Cyclohexene, **3a**											
ΔH_{3c-3b}	0.37	0.43	0.439	0.432	0.412	0.363	0.372	0.435	0.32(6)		
ΔH_{3c-3a}	-0.556	-1.000	-0.626	-0.483	-0.800	-0.708	-0.684	-0.584	-0.73(8)	-0.768, -0.746[48]	-0.70(13)[49]

3 Results and Discussion

3.1 Benchmark DFT calculations on DHA/VHF ground state isomerization reaction path

We start our analysis by benchmarking DFT energies of DHA/*s-trans*VHF isomerization. In Table 1, we show the results of the first set of benchmark calculations we performed on the DHA molecule shown in Figure 1. The structures **1a-e** are ordered from left to the right on the reaction coordinate on the figure. For many practical applications, the most significant quantities on the reaction path are the *s-trans*-VHF/DHA isomerization enthalpy, $\Delta H_{1e-1a} = H_{1e} - H_{1a}$ (=ΔH_1), and the back reaction barrier ΔH_{1b-1c} (ΔE_a). As discussed previously in Sec. 2, ΔH_1 must be larger than zero under vacuum conditions. Compared to the experimental results,[15] ΔH_1 is inaccurately predicted by the B3LYP and PBE functionals since B3LYP yields a negative ΔH_1 and PBE predicts DHA and *s-trans*-VHF to be almost iso-energetic.

Although these straightforward results are useful to understand which DFT functionals are more useful to further study DHA/VHF derivatives for example, they provide limited information regarding the source of DFT errors in these systems. Therefore we split the reaction path into two by investigating DHA/*s-cis*VHF and *s-cis*VHF/*s-trans*VHF isomerization energies separately. As shown in Figure 1, these two isomerization possess different chemical changes. While DHA/*s-cis*-VHF isomerization is a ring-opening isomerization, *s-cis*-VHF/*s-trans*-VHF isomerization is a cis-trans isomerization. Table 1 shows our results for the stability of DHA relative to *s-cis*-VHF, ΔH_{1a-1c}, stability of *s-cis*-VHF relative to *s-trans*-VHF, ΔH_{1c-1e} and also the back reaction barrier from

s-cis-VHF to DHA, $\Delta H_{1b-1c}(=E_a)$. We show that the variation among the DFT methods is less than 0.08 eV for ΔH_{1c-1e}, and when Hartree-Fock (HF) and Local Density Approximation (LDA) results are disregarded, this variation further reduces to 0.01 eV. All the DFT functionals yield *s-trans*-VHF to be more stable compared to *s-cis*-VHF. However, for ΔH_{1a-1c} the DFT results vary from 0.02 to 0.45 eV. In comparison, disregarding HF and LDA results does not change the outcome significantly, as the range becomes 0.02 to 0.43 eV. This suggests that for DHA/VHF isomerization, DFT functionals yield larger variations during the ring opening reaction as opposed to the cis-trans isomerization of VHF.

3.2 Correlation of DFT errors in ring-opening isomerizations

3.2.1 Cyclobutene and 1,3-cyclohexadiene

In Sec. 3.1, we have shown that the ΔH for ring opening isomerization (DHA/*s-cis*-VHF) leads to larger variations among the DFT results compared to the cis-trans isomerization between *s-cis*-VHF/*s-trans*-VHF. Although this result is useful to study the DHA/VHF isomerization further, understanding if these DFT errors persist in other compounds that undergo ring opening isomerization can be more useful for a larger scientific community. Although a large variety of photoswitches are known to undergo ring opening isomerizations, such as diarylethenes,[1] fulgides[3] and spiropyrans,[4] we focus on the ring opening isomerization in cyclobutene and 1,3-cyclohexadiene (Fig. 2). There are three main reasons for choosing cyclobutene and 1,3-cyclohexadiene over other compounds: 1) Cyclobutene and 1,3-cyclohexadiene motifs are present in many natural and synthetic compounds that undergo electrocyclization reactions,[54] therefore they can be studied as proxies for larger systems that undergo similar chemical changes. Electrocyclization reactions are the reverse of the ring opening reactions, where a π bond is broken and a σ bond is formed, hence the ring geometry is attained. These reactions can be classified based on the number of π electrons involved in the reaction. Therefore, cyclobutene and 1,3-cyclohexadiene can be considered as the most basic examples of 4π and 6π systems respectively. 2) Studying cyclobutene and 1,3-cyclohexadiene is not only efficient from the computational cost perspective, but it also removes any possible substitution effects on the ΔH, as these molecules are simple hydrocarbons. 3) Furthermore, ground state potential energy surface of cylobutene and 1,3-cyclohexadiene ring opening reactions have been studied extensively using experimental techniques, making it straightforward to evaluate the accuracy of the computational methods.

In Table 2, we show the ΔH obtained for several isomers of cyclobutene and 1,3-cyclohexadiene using DFT functionals. For both cyclobutene and cyclohexane, the ring opening isomerization occurs between ring (cyclobutene and 1,3-cyclohexadiene) and cis (*s-cis*-1,3-butadiene, **2b** and *s-cis*-1,3,5-hexatriene, **3b**) conformations. However, experimental ΔH for cyclobutene are only available between *s-trans*-1,3-butadiene, **2c**, and cyclobutene, whereas for 1,3-cyclohexadiene, it is available between 1,3-cyclohexadiene (**3a**), *s-cis*-1,3,5-hexatriene (**3c**) and *s-trans*-1,3,5-hexatriene.[47,49] Therefore, even though the ring opening occurs between the ring and *s-cis* conformations, in order to compare with the experiments, we study the *s-trans* (or *s-cis*) conformations as well. In Table 2, we show that ΔH_{2c-2b} and ΔH_{3c-3b} are predicted using different DFT functionals with almost uniform accuracy. These enthalpies correspond to cis-trans isomerizations and the result that we have in here is consistent with the result that we had for cis-trans VHF isomerization in Sec. 3.1. ΔH_{2c-2b} ranges between 0.13-0.16 eV, whereas ΔH_{3c-3b} ranges between 0.36-0.44 eV using different DFT methods. The DMC results for these reactions are 0.14(6) and 0.32(6) eV, respectively. However, for the trans to ring isomerization in cyclobutene, ΔH_{2c-2a}, we find that the DFT results vary between 0.20-0.64 eV. Similarly for cyclohexane DFT results vary between -0.57 to -1.09 eV for the cis to ring isomerization enthalpy, ΔH_{3c-3a}. Thus,

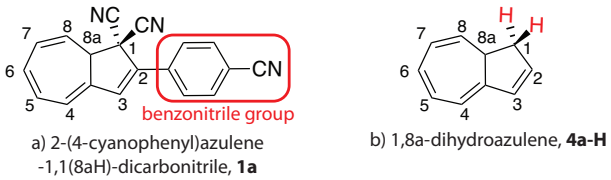

a) 2-(4-cyanophenyl)azulene -1,1(8aH)-dicarbonitrile, **1a**

b) 1,8a-dihydroazulene, **4a-H**

Figure 3: DHA derivatives that are used in this study, shown with the atom numbering on the DHA backbone. In (b), -H groups colored in red indicate the site of substitutions using the functional groups listed in Figure 5.

similar to the ring opening in the DHA-VHF isomerization, the ring opening reactions in cyclobutene and cyclohexane lead to a larger deviation between DFT results compared to cis/trans isomerizations.

3.2.2 DHA derivatives without the benzonitrile functional group

It is known that different functional groups on the DHA molecule can modify the isomerization enthalpies, especially the substitutions on the ring opening moiety.[13,14,24,26] In the **1a** derivative of DHA, there are two cyanide (-CN) functional groups in the ring opening moiety (On the carbon atom numbered as 1 in Figure 3a). Therefore, in order to eliminate effects of the substitution from the cyanide groups on the DHA molecule while making comparisons to cyclobutene and 1,3-cyclohexadiene, we examine a derivative of DHA, **4a-H**, where the two cyanide (-CN) groups on these carbon atoms are substituted with -H and the benzonitrile group is removed from the five membered carbon ring. The overall substitution scheme is shown in Figure 3a-b. We use the notation **4a-R**, where **-R** is the functional group used to substitute the -H atoms represented in red in Figure 3b. There are two main reasons for doing this: (1) we show that (in the SI), removing the benzonitrile group has only a small effect on the isomerization enthalpy, such that the isomerization enthalpy between DHA and *s-trans*-VHF conformations changes by less than 0.05 eV upon removing the benzonitrile functional group. (2) Performing CCSD(T) calculations on the DHA derivatives with the benzonitrile functional group takes significanly longer time, due to its unfavorable scaling, $O(N^7)$.

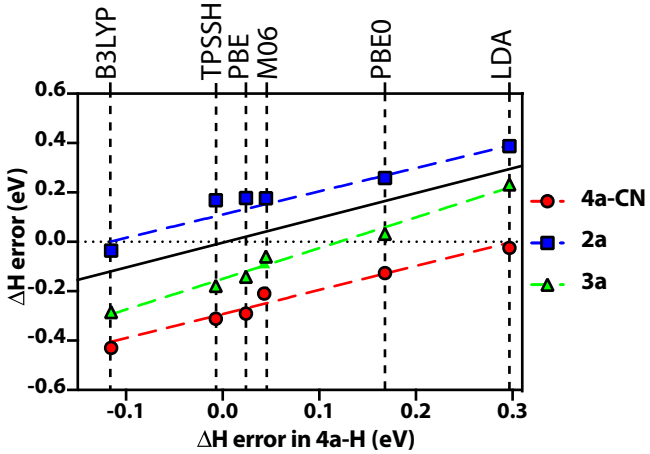

Figure 4: DFT errors in the isomerization enthalpy of -CN substituted DHA (**4a-CN**), cyclobutene and 1,3-cyclohexadiene, compared to the DFT errors in -H substituted DHA,(**4a-H**). Errors in DFT calculations are compared to the CCSD(T) method. Since the errors are systematic for the DFT methods, results for each DFT method is given on the dashed vertical lines. All results are given in eV.

3.2.3 Comparison of DFT errors in cyclobutene, 1,3-cyclohexane and DHA derivatives

We next investigate how the DFT errors in the ring opening isomerizations of DHA-VHF derivatives, cyclobutene and 1,3-cyclohexadiene correlate with each other. Figure 4 shows the errors of the DFT functionals for **4a-H** with respect to the CCSD(T) calculations. In Figure 4, there is a good correlation between the DFT functionals in the isomerization enthalpy for all the ring opening isomerization reactions considered here: the two DHA derivatives (**1a** and **4a-H**), cyclobutene and 1,3-cyclohexadiene. However, although the trends are very similar, all the errors have relative shifts with respect to each other. This result is important to show that no single DFT method is able to provide accurate energies when different carbon ring size and substitutions are considered for the same chemical reaction. For the **2a** derivative with 4 carbons on the ring, B3LYP is the most

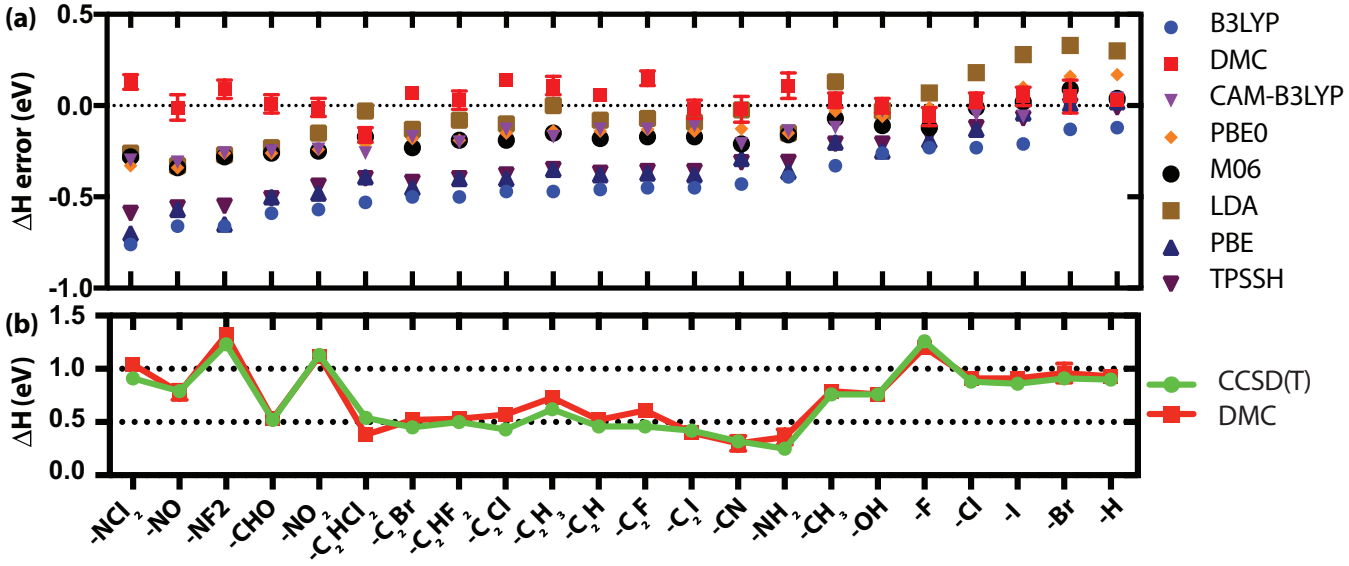

Figure 5: (a) Isomerization enthalpy, ΔH, error of DHA/VHF with substitutions on Carbon 1 site in Figure 3b compared to CCSD(T). (b) Isomerization enthalpy using CCSD(T) and QMC. All energies are given in eV.

accurate functional, whereas for the **3a** derivative with 6 carbons on the ring, PBE0 is the most accurate functional while B3LYP underestimates the isomerization enthalpy by nearly 0.3 eV. For the **4a-H** derivative, with 5 carbons on the ring, the errors of the DFT functionals are shown with the solid black line with the slope equal to 1 (corresponding to the x-axis), which is between the 4 carbon cyclobutene and 6 carbon 1,3-cyclohexadiene. Therefore, these results show that the energy of the *cis* isomer is overestimated (or the energy of the ring isomer is underestimated) with DFT methods, with increasing number of carbon atoms in the ring structure. However, the comparison between **4a-H** and **4a-CN** shows that the size of the carbon ring is not the only factor which influences the DFT results; the substituent on the ring opening moiety can be as important for introducing additional DFT errors.

3.3 Effect of the substitutions on DHA derivatives

In Sec. 3.2.1, we studied only two derivatives of DHA molecule, however it is important to study larger number of substitutions to clearly identify these trends in the DFT errors depending on the substitutions involved. Therefore, we perform 22 different substitutions on the ring opening carbon atoms, as given in the x-axes of Figures 5a-b, using the substitution scheme explained in Figure 3b. On the x-axis of Figure 5a and b, the compounds are listed with respect to isomerization enthalpy errors obtained using the B3LYP functional from left to right.

The errors with respect to the CCSD(T) method can be as large as 0.8 eV in the B3LYP or PBE functionals, e.g. for the -NCl_2 substitution. However, though smaller in magnitude, the errors in the isomerization other DFT functionals yield the same trend in the isomerization enthalpies. In comparison, CCSD(T) and QMC calculations results uniformly agree with each other, in Figure 5b, for all the substitutions investigated, with the largest difference among these two methods being nearly 0.1 eV. Figures 5a and b do not show any significant correlation between each other, meaning that large DFT errors are not a result of large isomerization enthalpies predicted using CCSD(T) or QMC method. However, the similarity between the errors in B3LYP, PBE and TPSSH[55] in Figure 5a is interesting to note, since these methods systematically underestimate the isomerization enthalpy.

3.4 Decomposition of the DFT energies

In Sec. 3.3 we identified that B3LYP, PBE and TPSSH functionals observe similar trends of errors in the isomerization enthalpies. In this section, we investigate the common qualities of these functionals to understand which components of the DFT Hamiltonians are responsible for these errors. Therefore, we investigate the breakdown of total energies in different DFT functionals.

Each DFT calculation using different functionals for a system yields different charge densities and geometric coordinates of the atoms at the end of the optimization. Therefore, the DFT errors can be a product of using different optimized charge densities, geometric coordinates of the atoms as well as the functionals representing the electron-electron interaction in DFT. In order to account for the contribution of each of these to the total error, ΔE, we write:

$$\Delta E = \Delta E_F + \Delta E_D + \Delta E_G \qquad (1)$$

where ΔE_F is the error due to the functional, ΔE_D is error due to the density and ΔE_G is the error due to the geometry.[56] In order to understand the extent that these elements contribute to the error in DFT calculations, we compare the DFT isomerization enthalpies for two cases: (1) with geometry and charge density optimized within each functional separately and (2) geometry and charge density optimized using the B3LYP functional only while they are calculated non self-consistently for the other functionals. We find that using B3LYP geometries and charge densities compared to optimizing each at every point on the reaction coordinate yields no more than 0.025 eV (3 meV/atom) difference (see SI for further details). Compared to the variations in the DFT total energies that can be as large as ∼0.6 eV (given in Figures 4 and 5a), ΔE_D and ΔE_G are rather small; therefore, we conclude that ΔE_F makes the largest contribution to ΔE. It has been discussed previously that different DFT approximations yield very similar charge densities, as exchange and correlation make up only a smaller part of the total energy composition, compared to classical interactions and hence their effect on the total charge density is minor in most cases.[56,57] However, this is a very active research area where it has also been shown that exchange correlation functionals that aim to satisfy a larger number of physical constraints can provide better charge densities, resembling that of higher accuracy methods.[58]

In Figure 6, we show how the exchange and correlation energies change upon isomerization from ring conformation to *s-trans* conformation in **4a-CN** and **4a-H**. There are two main conclusions that can be drawn from Figure 6: (1) the change in the correlation energy upon isomerization, ΔE_c, remains unchanged between the isomerization reactions of **4a-CN** and **4a-H** for all DFT functionals, except M06. However, in MP2, CCSD(T) and DMC calculations, we find that ΔE_c is larger for **4a-CN** compared to **4a-H**, indicating that correlation functionals of almost all DFT functionals are inaccurate. (2) For **4a-CN**, the exact exchange energy difference upon isomerization, ΔE_x, is substatially larger than other DFT exchange energy differences, indicating that -CN substitution may require a larger amount of exact exchange contribution for accurate results. However, local LDA exchange yields very similar ΔE_x as in HF for both **4a-CN** and **4a-H**. PBE, B3LYP and TPSSH exchange functionals on the other hand yield lower ΔE_x in both cases. The deficiency in the exchange component of these functionals can also explain the systematic behavior shown in Figure 5. The PBE exchange functional is based on LDA exchange with an enhancement factor that depends on the dimensionless density gradient parameter, s. The TPSSH functional uses a modified version of the PBE exchange with additional parametrization through the Laplacian of the charge density. However, it is known that the Generalized Gradient Exchange (GGA) exchange in TPSSH is designed to yield the same weak binding properties of PBE, such that TPSSH reproduces the exact PBE limit at the large s limit.[59] Hence, these errors could be attributed to the description of weak interactions in the PBE exchange functional.

For the case of B3LYP, we consider a breakdown of the functional Hamiltonian which can help to identify the components of the exchange functional leading to inaccurate results:[31]

$$E_{xc}^{B3LYP} = E_x^{LDA} + a_0(E_x^{HF} - E_x^{LDA}) + a_x(E_x^{B88} - E_x^{LDA}) + E_c^{LDA} - a_c(E_c^{LYP} - E_c^{LDA})$$

Where E_x^{LDA} is the local LDA exchange, E_x^{HF} is the exact exchange, E_x^{B88} is the Becke 88 exchange mixing, whereas E_c^{LDA} is the LDA correlation and E_c^{LYP} is the Lee-Par-Yang correlation functional. a_0, a_x and a_c represent mixing parameters, where for the B3LYP functionals they are 0.2, 0.72 and 0.81 respectively. In Figure 6, it is shown that ΔE_x for both HF and LDA is larger than B3LYP in the given DHA derivatives. Considering the B3LYP exchange is composed of HF, LDA and GGA exchange (B88), it can be expected that the GGA corrections should be responsible for lowering the ΔE_x in both reactions, hence lowering the ΔE_x in both reactions.

Therefore for B3LYP, our results suggest that the description of the GGA mixing to exchange energy must be adjusted to obtain accurate energy differences in ring opening reactions. In Figure 7, we perform several calculations varying the Becke88 exchange mixing, a_x, where $a_x = 0.72$ corresponds to the original B3LYP formulation. Throughout these calculations, we keep the exact exchange mixing constant, 0.2, therefore $a_x = 0.0$ means LDA exchange is 0.8, and there is no Becke 88 exchange contribution. For both cyclobutene and cyclohexane we find that a smaller amount of Becke 88 exchange, around $a_x = 0.6$ should suffice to find accurate ΔH for these isomerizations. However, for **4a-CN**, errors are more severe, such that even a smaller amount of Becke exchange must be used to obtain accurate ΔH and the optimal Becke 88 exchange mixing is found to be $a_x \approx 0.2 - 0.3$. In comparison to B3LYP exchange, CAM-B3LYP uses 0.19 HF and 0.81 B88 exchange for the short range, and 0.65 HF and 0.35 B88 exchange for the long range interactions. Therefore, using a larger portion of exact exchange for the weaker, long range interactions could help the CAM-B3LYP functional to yield a ΔE_x closer to the exact ΔE_x in HF. Having the same correlation energy as B3LYP, the difference in the CAM-B3LYP exchange functional leads to better total energies as given in Figure 6.

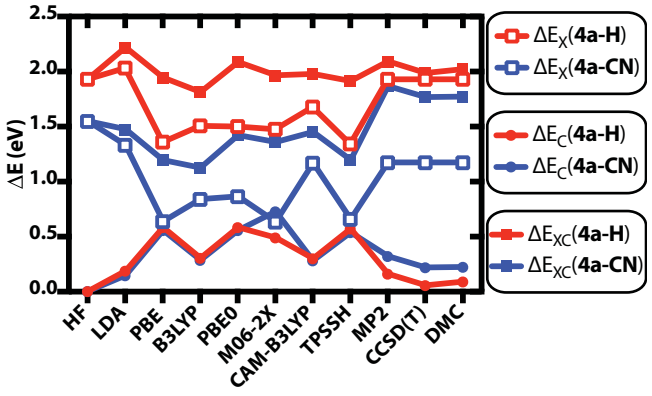

Figure 6: Changes in the exchange, ΔE_x, correlation, ΔE_c and exchange-correlation, ΔE_{xc}, energies upon ring opening isomerization from ring conformation to *s-trans* conformation in **4a-H** and **4a-CN**

3.5 Energy storage capacity of DHA derivatives

The substitutions performed on the DHA molcule given in Figure 5a-b not only help us identify the trends of errors in DFT calculations, depending on the substitutions, but it also identifies cases for which the isomerization enthalpies lead to large gravimetric energy densities suitable for solar thermal energy storage. For the substitutions considered, our QMC results show that the ΔH of DHA/*s-trans*-VHF varies between 0.38 to 1.32 eV. The **4a-NF$_2$** and **4a-F** derivatives have ring opening isomerization reaction enthalpies of 1.32 and 1.20 eV, respectively. These energies are larger than the ΔH of norbonadiene, 1.14 eV.[12] Further, the gravimetric energy storage capacities of **4a-F** and **4a-H** are 732 kJ/kg and 667 kJ/kg, respectively, which is larger then the value of highest

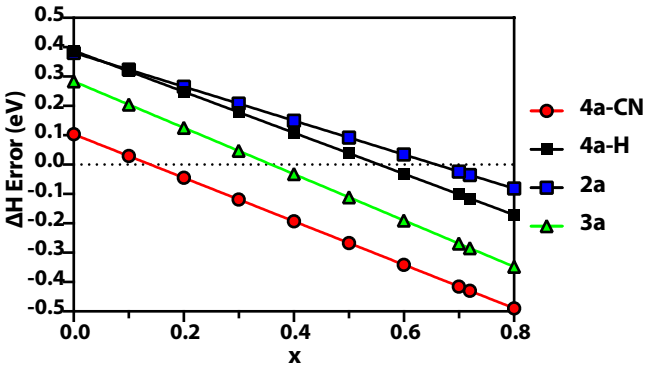

Figure 7: B3LYP errors in the ΔH of -CN substituted DHA, -H substituted DHA, cyclobutene and 1,3-cyclohexadiene as a function of Becke 88 exchange mixing parameter. DMC method is used as the reference. All results are given in eV.

energy density norbornadiene derivative, 636 kJ/kg.[5,12]

4 Conclusions

In this work, we are able to show that DFT approximations may fail to describe the thermochemistry of DHA/VHF ring opening isomerization reaction. We show that these are not only specific to the DHA/VHF couple, but very similar error patterns can also be found for cyclobutene and 1,3-cyclohexadiene and possibly in other ring opening isomerizations. We show that particularly B3LYP and PBE functionals predict qualitatively inaccurate relative stabilities in DHA-VHF isomerization, and mainly GGA exchange functionals in both functionals are responsible for the inaccurate results. However, the correct behavior of the correlation functional is equally important, as almost none of the DFT functionals investigated yield similar qualitative changes in the correlation energy upon the isomerization of DHA/VHF couple as in CCSD(T) and QMC calculations.

We find that DHA and VHF derivatives are promising alternatives for solar thermal energy storage applications, as the gravimetric energy density of the investigated molecules varies between 94-732 kJ/kg, which can be larger than the norbornadiene derivative. For all the DHA/VHF derivatives investigated, QMC and CCSD(T) isomerization energies agree with each other with a mean absolute error (MAE) of 0.07(1) eV/reaction.

Acknowledgement Calculations were performed in part at the National Energy Research Scientific Computing Center, which is supported by the Office of Science of the U.S. Department of Energy and in part by the National Science Foundation through Teragrid resources provided by TACC.

Supporting Information Available

Supporting information includes a comparison of DFT enthalpies of DHA/VHF isomerization at each DFT optimized geometries, effect of removing benzonitrile group n the isomerization enthalpy of DHA/*s-trans*-VHF and the effect of using polar solvents on the DFT DHA/VHF isomerization enthalpies.

References

(1) Irie, M. Diarylethenes for Memories and Switches. *Chem. Rev.* **2000**, *100*, 1685–1716.

(2) Browne, W. R.; Feringa, B. L. Making molecular machines work. *Nat. Nanotechnol.* **2006**, *1*, 25.

(3) Yokoyama, Y. Fulgides for Memories and Switches. *Chem. Rev.* **2000**, *100*, 1717–1740.

(4) Feringa, B. L.; Browne, W. R. Molecular Switches *Molecular Switches* **2011**, *1*, 1–792.

(5) Kucharski, T. J.; Tian, Y.; Akbulatov, S.; Boulatov, R. Chemical solutions for the closed-cycle storage of solar energy. *Energy Environ. Sci.* **2011**, *4*, 4449 – 4472.

(6) Kucharski, T. J.; Ferralis, N.; Kolpak, A. M.; Zheng, J. O.; Nocera, D. G.; Grossman, J. C. Templated assembly of

photoswitches significantly increases the energy-storage capacity of solar thermal fuels. *Nat. Chem.* **2014**, *6*, 441–7.

(7) Kolpak, A. M.; Grossman, J. C. Azobenzene-functionalized carbon nanotubes as high-energy density solar thermal fuels. *Nano Lett.* **2011**, *11*, 3156–3162.

(8) Zhitomirsky, D.; Grossman, J. C. Conformal Electroplating of Azobenzene-Based Solar Thermal Fuels onto Large-Area and Fiber Geometries. *ACS Appl. Mater. Interfaces* **2016**, *8*, 26319–26325.

(9) Cho, E. N.; Zhitomirsky, D.; Han, G. G.; Liu, Y.; Grossman, J. C. Molecularly Engineered Azobenzene Derivatives for High Energy Density Solid-State Solar Thermal Fuels. *ACS Applied Materials and Interfaces* **2017**, *9*, 8679–8687.

(10) Lennartson, A.; Roffey, A.; Moth-Poulsen, K. Designing photoswitches for molecular solar thermal energy storage. *Tetrahedron Lett.* **2015**, *56*, 1457–1465.

(11) Kuisma, M. J.; Lundin, A. M.; Moth-Poulsen, K.; Hyldgaard, P.; Erhart, P. Comparative Ab-Initio Study of Substituted Norbornadiene-Quadricyclane Compounds for Solar Thermal Storage. *J. Phys. Chem. C* **2016**, *120*, 3635–3645.

(12) Quant, M.; Lennartson, A.; Dreos, A.; Kuisma, M.; Erhart, P.; Børjesson, K.; Moth-Poulsen, K. Low Molecular Weight Norbornadiene Derivatives for Molecular Solar-Thermal Energy Storage. *Chem. - A Eur. J.* **2016**, *22*, 13265–13274.

(13) Hansen, M. H.; Elm, J.; Olsen, S. T.; Gejl, A. N.; Storm, F. E.; Frandsen, B. N.; Skov, A. B.; Nielsen, M. B.; Kjaergaard, H. G.; Mikkelsen, K. V. Theoretical Investigation of Substituent Effects on the Dihydroazulene/Vinylheptafulvene Photoswitch: Increasing the Energy Storage Capacity. *J. Phys. Chem. A* **2016**, *120*, 97829793.

(14) Broman, S. L.; Nielsen, M. B. Dihydroazulene: from controlling photochromism to molecular electronics devices. *Phys. Chem. Chem. Phys.* **2014**, *16*, 21172–82.

(15) Görner, H.; Fischer, C.; Gierisch, S.; Daub, J. J. Vinylheptafulvene photochromism: effects of substituents, solvent, and temperature in the photorearrangement of dihydroazulenes to vinylheptafulvenes. *J. Phys. Chem.* **1993**, *97*, 4110–4117.

(16) Boggio-Pasqua, M.; Bearpark, M. J.; Hunt, P. A.; Robb, M. A. Dihydroazulene/vinylheptafulvene photochromism: A model for one-way photochemistry via a conical intersection. *J. Am. Chem. Soc.* **2002**, *124*, 1456–1470.

(17) Rau, H.; Lueddecke, E. On the rotation-inversion controversy on photoisomerization of azobenzenes. Experimental proof of inversion. *Journal of the American Chemical Society* **1982**, *104*, 1616–1620.

(18) Yan, Y.; Wang, X.; Chen, J. I. L.; Ginger, D. S. Photoisomerization quantum yield of azobenzene-modified DNA depends on local sequence. *J. Am. Chem. Soc.* **2013**, *135*, 8382–8387.

(19) Pathem, B. K.; Zheng, Y. B.; Morton, S.; Petersen, M. Å.; Zhao, Y.; Chung, C.-H.; Yang, Y.; Jensen, L.; Nielsen, M. B.; Weiss, P. S. Photoreaction of Matrix-Isolated Dihydroazulene-Functionalized Molecules on Au{111}. *Nano Lett.* **2013**, *13*, 337–343.

(20) Broman, S. L.; Petersen, M. x.; Tortzen, C. G.; Kadziola, A.; Kilså, K.; Nielsen, M. B. Arylethynyl derivatives of the dihydroazulene/vinylheptafulvene photo/thermoswitch: Tuning the switching event. *J. Am. Chem. Soc.* **2010**, *132*, 9165–9174.

(21) Broman, S. L.; Petersen, A. U.; Tortzen, C. G.; Vibenholt, J.; Bond, A. D.; Nielsen, M. B. A Bis (

heptafulvenyl) -dicyanoethylene Thermoswitch with Two Sites for Ring Closure. *Org. Lett.* **2012**, *14*, 318–321.

(22) Schalk, O.; Broman, S. L.; Petersen, M. .; Khakhulin, D. V.; Brogaard, R. Y.; Nielsen, M. B.; Boguslavskiy, A. E.; Stolow, A.; Sølling, T. I. On the condensed phase ring-closure of vinylheptafulvalene and ring-opening of gaseous dihydroazulene. *J. Phys. Chem. A* **2013**, *117*, 3340–3347.

(23) Hansen, A. S.; MacKeprang, K.; Broman, S. L.; Hansen, M. H.; Gertsen, A. S.; Kildgaard, J. V.; Nielsen, O. F.; Mikkelsen, K. V.; Nielsen, M. B.; Kjaergaard, H. G. Characterisation of dihydroazulene and vinylheptafulvene derivatives using Raman spectroscopy: The CN-stretching region. *Spectrochim. Acta - Part A Mol. Biomol. Spectrosc.* **2016**, *161*, 70–76.

(24) Olsen, S. T.; Elm, J.; Storm, F. E.; Gejl, A. N.; Hansen, A. S.; Hansen, M. H.; Nikolajsen, J. R.; Nielsen, M. B.; Kjaergaard, H. G.; Mikkelsen, K. V. Computational methodology study of the optical and thermochemical properties of a molecular photoswitch. *J. Phys. Chem. A* **2015**, *119*, 896–904.

(25) Cacciarini, M.; Skov, A. B.; Jevric, M.; Hansen, A. S.; Elm, J.; Kjaergaard, H. G.; Mikkelsen, K. V.; Brøndsted Nielsen, M. Towards solar energy storage in the photochromic dihydroazulene-vinylheptafulvene system. *Chem. - A Eur. J.* **2015**, *21*, 7454–7461.

(26) Shahzad, N.; Nisa, R. U.; Ayub, K. Substituents effect on thermal electrocyclic reaction of dihydroazulene–vinylheptafulvene photoswitch: a DFT study to improve the photoswitch. *Struct. Chem.* **2013**, *24*, 2115–2126.

(27) Daub, J.; Knøchel, T.; Mannschreck, A. Photosensitive Dihydroazulenes with Chromogenic Properties. *Angew. Chemie Int. Ed. English* **1984**, *23*, 960–961.

(28) Hohenberg, P.; Kohn, W. The Inhomogeneous Electron Gas. *Phys. Rev.* **1964**, *136*, B864.

(29) Kohn, W.; Sham, L. J. Quantum density oscillations in an inhomogeneous electron gas. *Phys. Rev.* **1965**, *137*, A1697–A1705.

(30) Zhao, Y.; Truhlar, D. G. The M06 suite of density functionals for main group thermochemistry, thermochemical kinetics, noncovalent interactions, excited states, and transition elements: two new functionals and systematic testing of four M06-class functionals and 12 other functionals. *Theor. Chem. Acc.* **2008**, *120*, 215–241.

(31) Becke, A. D. Density-functional thermochemistry. III. The role of exact exchange. *J. Chem. Phys.* **1993**, *98*, 5648.

(32) Perdew, J. P.; Burke, K.; Ernzerhof, M. Generalized Gradient Approximation Made Simple. *Phys. Rev. Lett.* **1996**, *77*, 3865–3868.

(33) Ceperley, D. M.; Alder, B. J. Ground state of the electron gas by a stochastic model. *Phys. Rev. Lett.* **1980**, *45*, 566–569.

(34) Foulkes, W. M. C.; Mitas, L.; Needs, R. J.; Rajagopal, G. Quantum Monte Carlo simulations of solids. *Rev. Mod. Phys.* **2001**, *73*, 33–83.

(35) Shulenburger, L.; Mattsson, T. R. Quantum Monte Carlo applied to solids. *Phys. Rev. B* **2013**, *88*, 245117.

(36) Kobayashi, R. A direct coupled cluster algorithm for massively parallel computers. *Chem. Phys. Lett.* **1997**, *265*, 1–11.

(37) Adamo, C.; Barone, V. Toward reliable density functional methods without adjustable parameters: The PBE0 model. *J. Chem. Phys.* **1999**, *110*, 6158.

(38) Yanai, T.; Tew, D. P.; Handy, N. C. A new hybrid exchangecorrelation functional using the Coulomb-attenuating method (CAM-B3LYP). *Chem. Phys. Lett.* **2004**, *393*, 51 – 57.

(39) Chai, J.-D.; Head-Gordon, M. Long-range corrected hybrid density functionals with damped atom-atom dispersion corrections. *Phys. Chem. Chem. Phys.* **2008**, *10*, 6615–6620.

(40) Frisch, M. J.; Trucks, G. W.; Schlegel, H. B.; Scuseria, G. E.; Robb, M. A.; Cheeseman, J. R.; Scalmani, G.; Barone, V.; Mennucci, B.; Petersson, G. A. et al. Gaussian09 {R}evision {D}.01. 2009.

(41) Daub, J.; Gierisch, S.; Klement, U.; Knöchel, T.; Maas, G.; Seitz, U. Lichtinduzierte reversible Reaktionen: Synthesen und Eigenschaften photochromer 1,1-Dicyan-1,8a-dihydroazulene und thermochromer 8-(2,2-Dicyanvinyl)heptafulvene. *Chem. Ber.* **1986**, *119*, 2631–2646.

(42) Peng, C. Y.; Ayala, P. Y.; Schlegel, H. B.; Frisch, M. J. Using redundant internal coordinates to optimize equilibrium geometries and transition states. *J. Comput. Chem.* **1996**, *17*, 49–56.

(43) Møller, C.; Plesset, M. S. Note on an approximation treatment for many-electron systems. *Phys. Rev.* **1934**, *46*, 618–622.

(44) Truhlar, D. G. Basis set extrapolation. *Chem. Phys. Lett.* **1998**, *294*, 45–48.

(45) Valiev, M. NWChem: A Comprehensive and Scalable Open-Source Solution for Large Scale Molecular Simulations. *Comput. Phys. Commun.* **2010**, *181*, 1477.

(46) Universal solvation model based on solute electron density and on a continuum model of the solvent defined by the bulk dielectric constant and atomic surface tensions. *J. Phys. Chem. B* **2009**, *113*, 6378–6396.

(47) Barborini, M.; Guidoni, L. Reaction pathways by quantum Monte Carlo: Insight on the torsion barrier of 1,3-butadiene, and the conrotatory ring opening of cyclobutene. *J. Chem. Phys.* **2012**, *137*, 224309.

(48) Data from NIST Computational Chemistry Comparison and Benchmark Database. CCSD(T) calculations are performed at CCSD(T)// MP2FC/6-31G* level. http://cccbdb.nist.gov/.

(49) Estimated using heat of formations of 1,3-butadiene (H_f=26.00 ± 0.19 kcal/mol and 26.75 ± 0.23 kcal/mol), ethylene (H_f=12.54 kcal/ mol), and cyclohexene (H_f= -1.03 ± 0.23 kcal/mol). Data from NIST Standard Reference Database. http://webbook.nist.gov/chemistry.

(50) Drummond, N. D.; Towler, M. D.; Needs, R. J. Jastrow correlation factor for atoms, molecules, and solids. *Phys. Rev. B - Condens. Matter Mater. Phys.* **2004**, *70*, 1–11.

(51) Needs, R. J.; Towler, M. D.; Drummond, N. D.; López Ríos, P. Continuum variational and diffusion quantum Monte Carlo calculations. *J. Phys. Condens. Matter* **2010**, *22*, 023201.

(52) Burkatzki, M.; Filippi, C.; Dolg, M. Energy-consistent pseudopotentials for quantum Monte Carlo calculations. *J. Chem. Phys.* **2007**, *126*, 234105.

(53) Casula, M.; Moroni, S.; Sorella, S.; Filippi, C. Size-consistent Variational Approaches to Nonlocal Pseudopotentials: Standard and Lattice Regularized Diffusion Monte Carlo Methods Revisited. *J. Chem. Phys.* **2010**, *132*, 154113.

(54) Beaudry, C. M.; Malerich, J. P.; Trauner, D. Biosynthetic and biomimetic electrocyclizations. *Chem. Rev.* **2005**, *105*, 4757–4778.

(55) Staroverov, V. N.; Scuseria, G. E.; Tao, J.; Perdew, J. P. Comparative assessment

of a new nonempirical density functional: Molecules and hydrogen-bonded complexes. *J. Chem. Phys.* **2003**, *119*, 12129–12137.

(56) Kim, M. C.; Sim, E.; Burke, K. Understanding and reducing errors in density functional calculations. *Phys. Rev. Lett.* **2013**, *111*, 73003.

(57) Cohen, A. J.; Mori-Sanchez, P.; Yang, W. Challenges for density functional theory. *Chem. Rev.* **2012**, *112*, 289–320.

(58) Medvedev, M. G.; Bushmarinov, I. S.; Sun, J.; Perdew, J. P.; Lyssenko, K. A. Density functional theory is straying from the path toward the exact functional. *Science* **2017**, *355*, 49–52.

(59) Tao, J.; Perdew, J. P.; Staroverov, V. N.; Scuseria, G. E. Climbing the Density Functional Ladder: Nonempirical Meta˘Generalized Gradient Approximation Designed for Molecules and Solids. *Phys. Rev. Lett.* **2003**, *91*, 146401.